Food Chemistry 112 (2009) 162–168

Contents lists available at ScienceDirect

Food Chemistry

journal homepage: www.elsevier.com/locate/foodchem

Raman analysis of *surimi* gelation by addition of wheat dietary fibre

Ignacio Sánchez-González [a], Arantxa Rodríguez-Casado [b], Mercedes Careche [a,*], Pedro Carmona [c]

[a] *Instituto del Frío – CSIC. c./José Antonio Novais 10, 28040 Madrid, Spain*
[b] *IMDEA Alimentación, 28049 Madrid, Spain*
[c] *Instituto de Estructura de la Materia – CSIC. c./Serrano 121, 28006 Madrid, Spain*

ARTICLE INFO

Article history:
Received 16 November 2007
Received in revised form 27 March 2008
Accepted 16 May 2008

Keywords:
Surimi
Surimi gels
Dietary fibre
Protein structure
Raman spectroscopy
Interactions

ABSTRACT

Raman analysis has been carried out to study the effects of Vitacel® wheat dietary fibre (WDF) during gelation of *surimi*. The main results reveal the following: (a) Vitacel® comprises natural cellulose I as major component; (b) hydration of WDF leads to νCH frequency upshifting and decreasing intensity. On the basis of these spectral features it is suggested that water transfer from protein to WDF can occur in *surimi* gels. WDF hydration can be interpreted in the sense that this fibre either takes water that is delivered from the gel protein upon heat-mediated formation of β-sheets and hydrophobic contacts and/or or acts as an active dehydrating agent. An increase of solvent-exposed hydrophobic side chains is observed in the sol phase, upon the addition of WDF, which may cause breaking of intermolecular protein hydrophobic contacts; a subsequent change upon WDF-containing gel formation is the reduction in the νCH intensity, which may be indicative of increasing hydrophobic WDF-protein contacts. Interestingly, these results constitute molecular data, to be considered when designing restructured fish products with these fibre ingredients.

1. Introduction

Dietary fibres (DF) have a positive association for consumers as a functional ingredient, and the scientific evidence for their beneficial health effects are well-known (Dreher, 2001; Gallaher, 2000). DF is at least quantitatively the principal ingredient used in functional foods (Saura-Calixto & Goñi, 2005). Wheat dietary fibre (WDF) is insoluble, neutral in taste and odour and has been used, for example, in formulations of restructured fish products (Sánchez-Alonso, Haki-Maleki, & Borderías, 2007). This fibre, like other biopolymers, can also be used technologically as a water-controlling agent, in order to obtain desirable textures, physical stability and thus contribute to the final characteristics of the formulated foods (Lee, 2002; Sánchez-Alonso, Haki-Maleki, & Borderías, 2006).

Surimi technology allows the formulation of tailor-made seafood products, which can be considered as excellent carriers of some functional ingredients, provided they do not completely interfere with the gelation of the myofibrillar proteins. The presence of WDF in *surimi* gels leads to changes in the rheological properties of these products (Sánchez-González, 2008). When WDF is incorporated into the formulation, an increase of initial and residual stress, elastic and viscous moduli can be observed at equal *surimi* (and therefore protein) concentrations. However, if the WDF is added at equal water concentrations, that is, replacing part of the *surimi* (or protein) by WDF, the rheological parameters mentioned above may not reach the values obtained with the control. The above results suggest that the effect of WDF addition on the formulations could be a balance of (a) the strengthening effect of the fibre on the gel structure either by acting as a filler or by its high water absorbing capacity and (b) the increase of the heterogeneity of the protein network, maybe due to the aggregation/coagulation of the surrounding protein matrix.

One way to study the molecular interactions between biopolymers and proteins in the above models is the use of Raman spectroscopy. This technique gives information based on both the relative intensities and the frequencies of vibrational motions on the amino acid side chains, polypeptide and polysaccharide backbone. It has been proposed as a useful tool to investigate molecular interactions, structural changes in proteins and water in seafood products during storage (Careche, Herrero, Rodríguez-Casado, Del Mazo, & Carmona,1999; Herrero, Carmona, & Careche, 2004), as well as in the study of the alterations in protein side chains and secondary structure in *surimi*, gels, or during gelation of actomyosin (Bouraoui, Nakai, & Li-Chan, 1997; Sánchez-González et al., 2008; Thawornchinsombut, Park, Meng, & Li-Chan, 2006). It has also been used in the study of the structure of celluloses (Proniewicz et al., 2001). The changes from *surimi* to gels in relation to protein structures include increase of hydrophobic interactions, decreasing of α-helical structure and concomitant increasing of

Abbreviations: DF, dietary fibre; WDF, wheat dietary fibre.

* Corresponding author. Tel.: +34 91 549 2300; fax: +34 91 549 3627.
E-mail address: mcareche@if.csic.es (M. Careche).

0308-8146/$ - see front matter © 2008 Elsevier Ltd. All rights reserved.
doi:10.1016/j.foodchem.2008.05.054

β-sheets, this transition involving rearrangement of protein hydrogen bonding (Bouraoui et al., 1997; Sánchez-González et al., 2008).

This work is focused on the Raman analysis of Vitacel® WDF and its effects on the structural changes of *surimi* proteins during gelation. This investigation is targeted to understand the WDF-protein interactions leading to different mechanical and textural properties in the presence of this fibre.

2. Experimental

2.1. Materials

Frozen blocks of Alaska Pollack (*Theragra chalcogramma*) *surimi* (grade FA) from the North Pacific were obtained from the company Angulas Aguinaga S.A., Spain, and stored at −20 °C prior to use (6–9 months after capture date). The shelf life of these lots was 18–20 months at a maximum temperature of −18 °C. Wheat fibre Vitacel® WF200, with average fibre length of 250 μm, consisting of 74% cellulose, 26% hemicellulose and <0.5% lignin was acquired from Campi y Jové S.L. (Barcelona, Spain) and maintained at 10 °C in the absence of air. According to the manufacturer, this fibre contained maximum moisture and ash contents of 8% and 3%, respectively, 0.4% protein, 0.2% fat and a pH value of 6.5 ± 1.5 at a 10% suspension.

2.2. Surimi gel preparation

Surimi was partially thawed at room temperature for 1 h. Approximately 800 g were cut in small pieces, chopped in a vacuum cutter (Stephan Universal Machine UM5, Stephan u. Söhne GmbH & Co., Hameln, Germany) for 2.5 min, and mixed for another 2.5 min with enough NaCl, in order to obtain 2.5% in the final product. A dispersion of WDF in water was added in order to obtain WDF products having 3% and 6% WDF, at a final moisture content of 74.5%. Formulations without WDF having 17%, 14% and 11% protein (74.5%, 77.5%, and 80.5% moisture) were prepared as controls. The temperature was kept below 10 °C during the process. A portion of this *surimi* paste (sol) was separated for Raman analyses and stored at 2 °C prior to analysis (∼15 h). The remaining sol was stuffed into polyvinylidine casings (Amcor Flexibles Barcelona, Spain) and subjected to heating at 90 °C for 50 min in a water bath to obtain the gels. They were cooled in iced water and stored at 2.0 °C for ∼12 h before analysis. Four to six gels of about 190 g (35 mm diameter and ∼15 cm length) were obtained and used for subsequent analyses.

The *surimi* used was from the same batch. Each gel formulation (0%, 3% or 6% fibre) was prepared on separate days as well as the replicates (×3) for each formulation. Thus 9 different gel preparations were prepared on 9 different days. The gel scores (ranking from 5 to 0, highest to poorest quality), according to the folding test (Lanier, Hart, & Martin, 1991), were for 0%, 3% and 6% WDF-containing formulations: 5.0 ± 0.0a; 4.8 ± 0.2ab, and 3.3 ± 1.2b, respectively (mean score values of seven assessors; different letters indicate significant differences). Other data referring to ultrastructure and rheological analysis of these formulations will be published elsewhere (Sánchez-González, 2008).

2.3. Water retention capacity of the fibre

Water retention capacity was measured following the method of Robertson and Eastwood (1981). Water (10 ml) was added to the WDF, which was allowed to stand overnight at room temperature, and centrifuged at 3000g for 20 min at room temperature. Water retention capacity was expressed as grams of water retained per gram of dry sample. Measurements were made in triplicate.

2.4. Raman spectroscopy

Samples of Alaska Pollack *surimi*, sol and gels were transferred to glass tubes (5.0 cm height and 5.0 mm i.d; Wilmad Glass Co., Inc., Buena, NJ). Spectra were excited with a 1064 nm Nd:YAG laser line and recorded on a Bruker RFS 100/S FT spectrometer (Bruker, Karlsruhe, Germany). The scattered radiation was collected at 180° to the source, and the frequency-dependent scattering of the Raman spectra that occurs with this spectrometer was corrected by multiplying point by point $(\nu_{laser}/\nu)^4$. The samples thermostatted at 15–20 °C were illuminated with 290 mW laser power. Two thousand scans were recorded for every three portions from the same sample, each sample consisting of 6000 scans. Raman spectra were resolved at 4.0 cm^{-1} resolution with a liquid nitrogen-cooled Ge detector. Frequency measurements are accurate to ±0.5 cm^{-1}. Spectra were processed and evaluated using Grams/AI (Thermo Fisher Scientific, Inc., Waltham, MA) and Opus 2.2. (Bruker) software. Amide I band (around 1650 cm^{-1}) was used in order to estimate the protein secondary structure and was analysed according to literature methods (Alix, Pedanou, & Berjot, 1988; Careche, Herrero, Rodríguez-Casado, Del Mazo, & Carmona, 1999). Each spectrum was normalised to the intensity of the phenylalanine band centred at 1003 ± 2 cm^{-1} and considered to be unaffected by environment. Amino acid side chains bands such as tryptophan and tyrosine doublet were analysed according to the method described in Careche et al., (1999). For the analysis of νCH band centred at 2935 cm^{-1} it was necessary to first subtract the CH band of WDF whenever this ingredient was present. For this purpose, a spectrum of WDF aqueous dispersions with 74.5% moisture content, treated in the same conditions as the *surimi* sols or gels, was subtracted until the C–O ring stretching modes of the cellulose (near 1095 cm^{-1}) were no longer visible (Wiley & Atalla, 1987). The study of the effect of the protein matrix over the WDF in the sol and gel was performed by subtracting the spectra of the sols or gels without fibre at 11% protein concentration from those containing 6% WDF until the 1003 cm^{-1} Phe band was annulled. The 1095 cm^{-1} band was used as internal standard for measurements of normalised intensities of the 2895 cm^{-1} νCH band (Wiley & Atalla, 1987).

2.5. Statistical analysis

A two-way analysis of variance was performed as a function of type of sample (*surimi*, sol and gel) and fibre content (0%, 3%, 6%) on the protein secondary (% α-helix, β-sheet, turns and random coil) and tertiary (tyrosine doublet, νCH stretching and δCH_2 bending bands) structure. Then, a one way analysis of variance was done separately for the sol and for the gels as a function of fibre concentration. The Levene test was used to check the equality of variances. Where variances were equal, the difference between means was analysed by the Bonferroni test. Where equality of variances could not be assumed, a Tamhane T2 test was used. One way analysis of variance was also used for the study of the differences of the νCH band of the fibre at different moisture contents and within the sol and gel. The statistical package used was SPSS 13 (SPSS Inc., Chicago, IL) and significance was established at $P \leqslant 0.05$. Results were expressed as average ± standard error of the mean (SEM).

3. Results and discussion

3.1. WDF Raman spectroscopy characterisation

WDF is a naturally-occurring complex polymer material and its macromolecular substances comprise mainly cellulose, hemicellulose

and lignin. It is necessary to characterise the chemical structure of the WDF used in this work by comparison with WDF components to understand their contributions. In this connection, the Raman analysis of WDF is summarised in Table 1 and through the following figures.

The 2600–3550 cm^{-1} region (Fig. 1) is dominated by cellulose through its strong band located at 2895 cm^{-1} and the shoulders at 2945 and 2966 cm^{-1} (Proniewicz et al., 2001; Shen, Rahiala, & Rosenholm, 1998), and the weak band at 2986 cm^{-1} coincides with hemicellulose as shown in Table 1. Those shoulders become visible upon suspension in water (Fig. 1), because the intensity and masking caused by the predominant 2895 cm^{-1} νCH vibration decreases. In addition, this band slightly shifts towards higher frequencies (2897 cm^{-1}) upon hydration. The factors influencing the intensity of νCH infrared and Raman bands have been studied and the use of these intensities as a tool for chemical diagnosis has been suggested. According to some literature works dealing with hydrogen bonding of water with molecules having CH bonds that are contiguous to oxygen atoms (Barnes, 2004; Gussoni & Castiglioni, 2000; Mizuno, Imafuji, Fujiwara, Ohta, & Tamiya, 2003), the origin of the above frequency upshifting and decrease of the νCH intensity can be explained through binding of a hydrogen bond donor to the lone electron pairs of the glucose oxygen atoms. In fact, in the absence of the said hydrogen bonding, electronic charge is back-donated from the oxygen lone electron pairs to the σ^* orbital of a contiguous CH bond. The increase of electronic charge in the σ^*_{CH} orbital makes the CH bond weaker, with subsequent decrease of the νCH frequency and intensity increase. Therefore, the opposite is expected when fixing the oxygen electron pairs through hydrogen bonding (Gussoni & Castiglioni, 2000). Some δCH bands of WDF also shift to higher frequency side upon hydration, as described below, which implies that their respective CH groups are subjected to attractive interactions with water molecules by involving the so called blue-shifting C–H···O hydrogen bonding

Table 1
General band assignments of FT-Raman peaks of dried WDF based on literature (Agarwal & Ralph, 1997; Shen et al., 1998; Wiley & Atalla, 1987; Zhbankov et al., 2002)

Band	Wavenumber (cm^{-1})	Assignment
0	378 m	Cellulose C–C–C, C–C–O bend
1	436 m	Cellulose C–C–C, C–C–O bend
2	459 w	Cellulose C–C–C, C–C–O bend
3	492 w	Hemicellulose C–C–C, C–C–O bend
4	519 sh	Cellulose C–C–C, C–C–O bend
5	535 vw	Hemicellulose C–C–C, C–C–O bend
6	899 m	Cellulose HC–C, HC–O in C-6 bend
7	970 w	Cellulose C–C, C–O stretching
8	997 w	Cellulose C–C, C–O stretching
9	1040 sh	Cellulose C–C, C–O stretching
10	1058 sh	Cellulose C–C, C–O stretching
11	1095 s	Cellulose C–C, C–O stretching
12	1120 s	Cellulose C–C, C–O stretching
13	1151 m	Cellulose C–C, C–O stretching
14	1204 vw	Cellulose C–C, C–O stretching
15	1248 vw	Hemicellulose HC–C, HC–O bend
16	1266 vw	Cellulose HCC, HCO, HOC bend
17	1318 sh	Hemicellulose HCC, HCO, HOC bend
18	1339 w	Cellulose HCC, HCO, HOC bend
19	1379 m	Cellulose HCC, HCO, HOC bend
20	1415 w	Cellulose HCC, HCO, HOC bend
21	1466 m	Cellulose HCC, HCO, HOC bend
22	2735 w	
23	2895 vs	Cellulose C–H stretching
24	2945 sh	Cellulose C–H stretching
25	2966 sh	Cellulose C–H stretching
26	2986 sh	Hemicellulose C–H stretching
27	3225 vs	O–H stretching

Abbreviations: s, strong; vs, very strong; m, medium; w, weak; vw, very weak; sh, shoulder; ν, stretching; and δ, deformation.

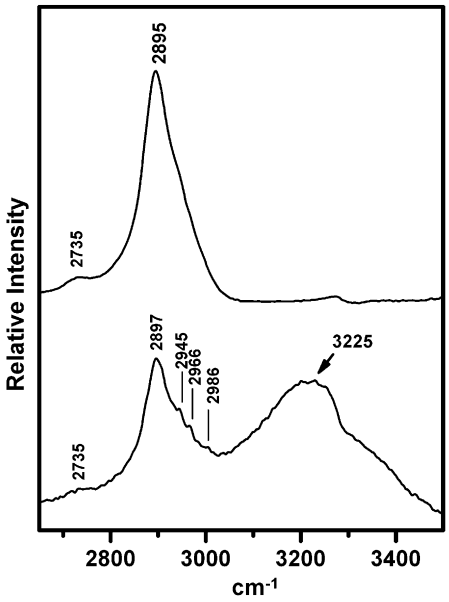

Fig. 1. The averaged Raman spectra in the 2600–3550 cm^{-1} region (C–H νCH and νOH region) of dried WDF (upper) and in WDF aqueous suspension with 74.5% water (lower).

(Mizuno et al., 2003). On the above basis it is expected that some bands of δCH_2, δCOH and δCCH character located in the 1300–1500 cm^{-1} range shift towards higher frequencies upon hydration. This indeed occurs for the bands located at 1466, 1415, 1318 and 1266 cm^{-1} (Fig. 2A). However, the hydration of WDF does not seem to affect the νCO and/or νCC vibrations falling in the 800–1200 cm^{-1} range as reflected in Fig. 2B, which supports the use of the medium intensity 1095 cm^{-1} band as internal standard for measurements of normalised intensities (Wiley & Atalla, 1987). Hemicellulose is visible through the weak band located at 1318 cm^{-1} (Agarwal & Ralph 1997; Shen et al., 1998) which shifts towards higher frequencies upon hydration; the remaining spectral profile in the 800–1700 cm^{-1} range is dominated by bands of cellulose.

In the 300–800 cm^{-1} range several, closely spaced, medium intensity bands are observed in the Raman spectrum (Fig. 3). Calculations of vibrational modes of cellulose show that the modes below 800 cm^{-1} are to a large extent delocalised, indicating that the vibrational modes are quite complex (Wiley & Atalla, 1987) (Table 1). The predominant vibrational characters are δCCO and δCCC which generate a prominent band at 378 cm^{-1}, corresponding to natural cellulose I (Zhbankov et al., 2002), as the major component of WDF.

3.2. Spectral characterisation of the matrix

3.2.1. Changes in the fibre

The averaged Raman spectra in the 2800–3000 cm^{-1} region of WDF with 74.5% of water and the difference spectrum of WDF from *surimi* gel containing 6% WDF show a lowering of the νCH intensity in the matrix, as well as a blue-shifting of the νCH band (Fig. 4), thus suggesting hydration of the fibre within the gel. This 3 cm^{-1} shifting of the WDF νCH band toward higher frequencies can be considered as blue-shifting for the following reasons. Firstly, the frequency measurements are accurate to ±0.5 cm^{-1}, as described in the Experimental section. Secondly, the νCH frequency change corresponds to an order of magnitude, which is the same as that from other molecules showing νCH frequency blue-shifting upon hydrogen bond interactions with water (Mizuno et al., 2003). In

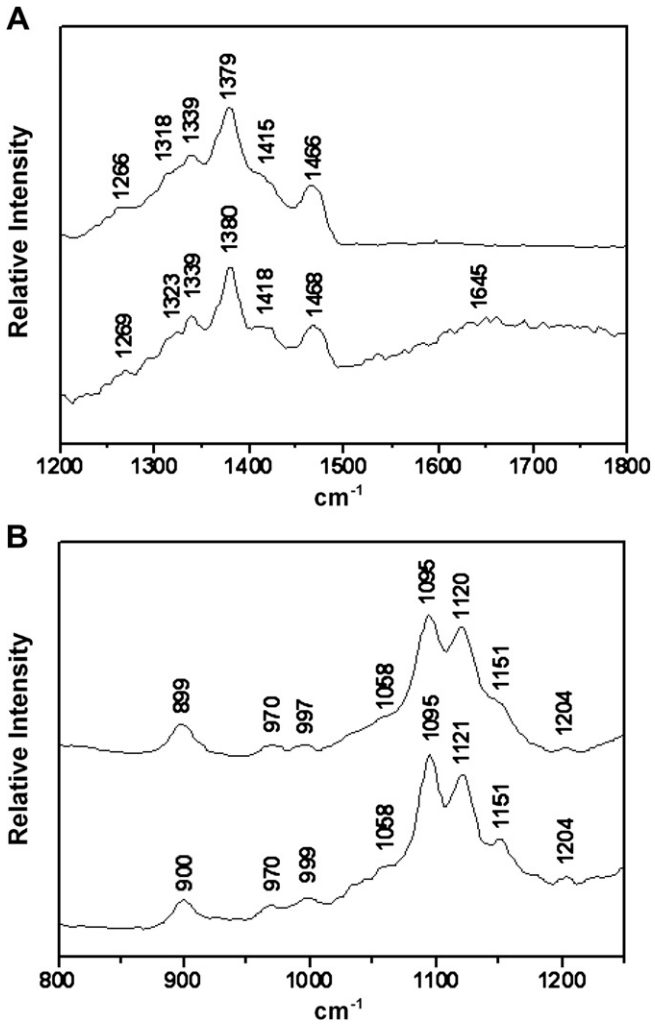

Fig. 2. The averaged Raman spectra in the 1200–1800 cm^{-1} range (A) and 800–1250 cm^{-1} range (B) of dried WDF (upper) and WDF aqueous suspension with 74.5% moisture (lower).

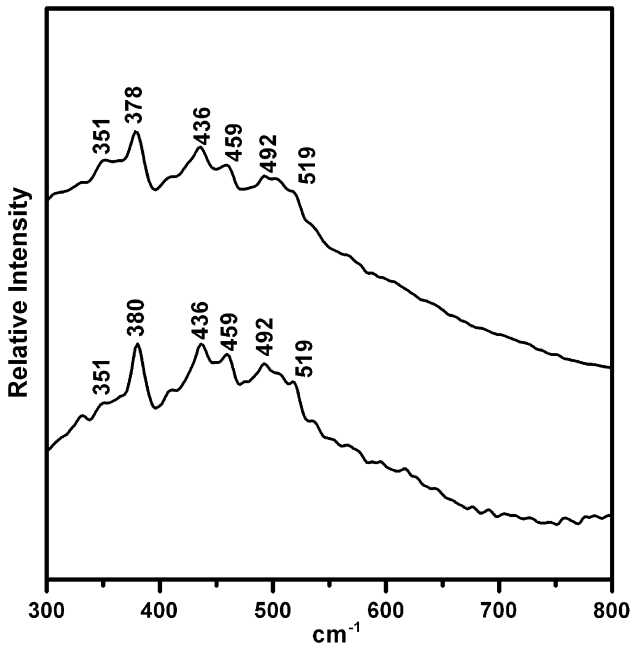

Fig. 3. The averaged Raman spectra in the 300–800 cm^{-1} range of WDF dried (upper) and WDF aqueous suspension with 74.5% moisture (lower).

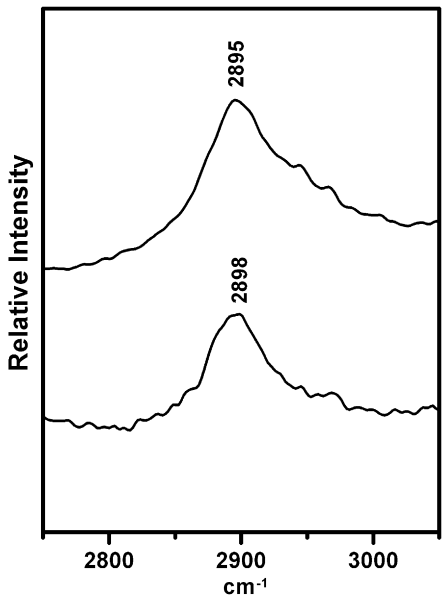

Fig. 4. The averaged Raman spectra in the 2750–3050 cm^{-1} region of WDF with 74.5% of water content (upper) and the difference spectrum of WDF from *surimi* gel containing 6% WDF (lower).

order to quantify our spectroscopic results, we measured the normalised intensity of the νCH band of aqueous suspensions of WDF as a function of the water content of the sample up to the maximum water retention capacity of the fibre, which was 6.7 g water/g dry fibre (87% moisture). Fig. 5 shows that this intensity decreases with increasing moisture. No changes were observed in this band as a function of heating (not shown). Interestingly, the normalised intensity of the νCH band in the WDF difference spectrum from gel containing 6% WDF and 74.5% moisture is lower than that of pure WDF in water at the same moisture (Fig. 5). All of these results suggest that wheat dietary fibre has taken a certain amount of gel water, leading to higher local moisture surrounding the wheat fibre. By contrast, no visible changes appeared in the WDF-containing sols and we can assume that the moisture of the fibre before heating corresponds to the average moisture of the matrix (Fig. 5).

Below 1800 cm^{-1}, small spectral changes in gels were found for bands of δCH_2, δCOH and δCCH character, located in the 1300–1500 cm^{-1} range, which were similar to those described above for isolated WDF with increasing moisture.

3.2.2. Changes in the protein

The normalised intensity of the amide I band of the gel matrix did not change as a function of protein concentration in the absence of fibre, but the relative intensity of the νCH band centred at 2935 increased slightly at decreasing moisture content (not shown). Thus, only in the latter band, the protein concentration effect was corrected when analysing the effect of WDF.

Fig. 6 includes the difference Raman spectrum of *surimi* gel containing WDF, compared with pure gel, and shows that amide I band of gel matrix is shifted towards higher frequencies upon addition of WDF. This frequency upshifting can be interpreted in terms of an increase of β-sheets caused by the fibre addition, according to spectrum-structure correlation (Careche et al., 1999). The interpretation of this spectral change is supported by the amide III region, where a more pronounced β-sheet shoulder at 1238 cm^{-1} is appar-

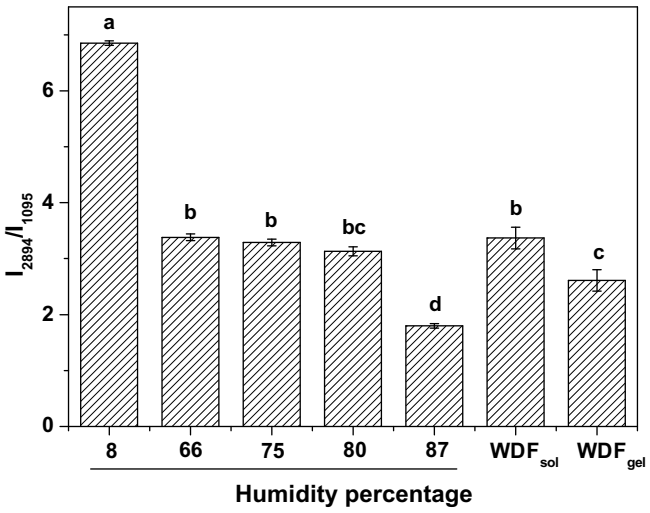

Fig. 5. Bar diagram showing the intensity ratio (I_{2894}/I_{1095}). The WDF_{sol} and WDF_{gel} bars correspond to the 2894 cm^{-1} relative intensity of WDF within sol and gel matrices having 74.5% average moisture. The other bars correspond to WDF aqueous suspensions having 8%, 66%, 75%, 80%, and 87% moisture. Error bars indicate standard error of the mean.

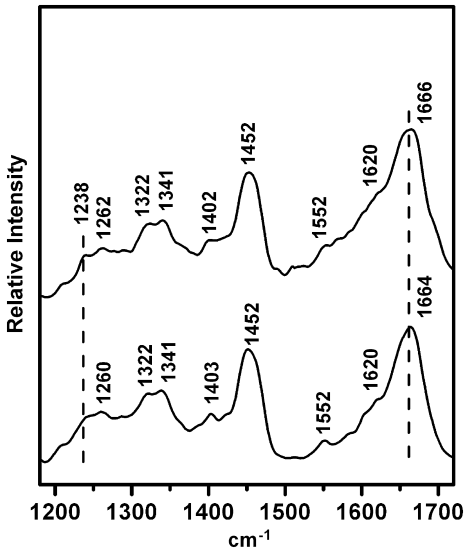

Fig. 6. The averaged Raman spectra obtained from *surimi* gels. Difference spectrum of gel with 6% WDF upon subtraction of WDF (upper), and control gel (lower).

ent in the spectrum of the gel containing WDF (Fig. 6). A quantitative analysis of the amide I band in the gels reveals a significant increase of β-sheet proportion with increasing content of WDF, which is accompanied by a trend of decreasing content in α-helices. No significant changes were noticed in relation to the sol samples (Fig. 7). As regards turns and unordered protein structures, there were no significant differences in the sols nor in the gels (not shown).

A positive relation on the proportion of β-structures in conditions of higher elasticity and therefore, more regular arrangement of the protein network has been suggested (Niwa & Nakajima, 1975). However, as the temperature is increased during cooking, coagulation of proteins also takes place, resulting in a release of a portion of water from the random coil peptide carbonyl group and formation of β-sheet upon heating to high temperature (Niwa, 1992). Thus, the β-structures are associated to both nonspecific coagulation consisting of aggregates and to protein network

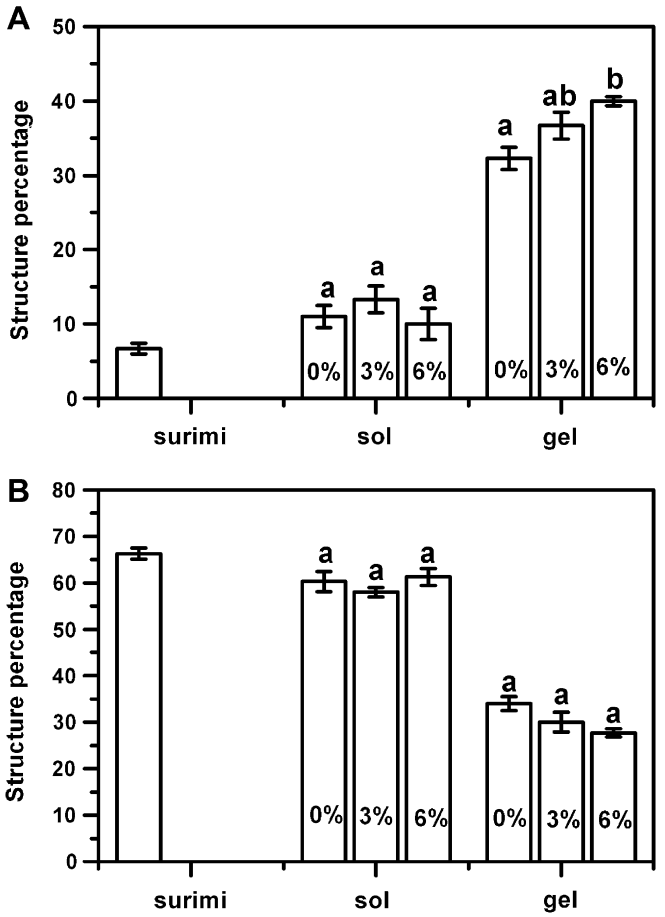

Fig. 7. Bar diagram corresponding to β-sheet (A) and α-helix (B) content during gelation with 0%, 3% and 6% WDF at 74.5% moisture content. Bars with different letters in the same phase mean significant differences ($P < 0.05$). Error bars indicate standard error of the mean.

formation. In proteins other than myofibrillar, there is also evidence of dehydration of proteins accompanied by β-sheet aggregation, viewed as nonspecific coagulation (Al-Azzam et al., 2002; Van de Weert, Haris, Hennik, & Crommelin, 2001). Taking into account these data, we dehydrated a *surimi* sample toward 68% moisture which would fall within the moisture range that the *surimi* matrix would have if the local hydration of the WDF were around 84% (Fig. 5). The gel prepared from this dehydrated *surimi* generated a β-sheet content which was very close to that found in *surimi* gel containing 6% WDF (not shown). That means that the β-sheet content generated by WDF addition can be explained from the viewpoint of a protein matrix dehydration. The role of WDF, either as an active dehydrating agent of gel protein matrix and/or acceptor of the water released from this matrix upon β-structure formation, is consistent with data from Fig. 5.

As to the protein tertiary structure, the most visible changes correspond to the νCH profile (I_{2935}/I_{1003}), whose intensity increases in the sol phase upon addition of WDF (Fig. 8). According to work carried out using model biomolecules this increase in intensity is caused by breaking of hydrophobic contacts between protein side chains, such as those of leucine, which become solvent-exposed (Carmona, Molina, & Rodríguez-Casado, 2003; Rader, Hespenheide, Kuhn, & Thorpe, 2002). The absence of local hydration changes in the sols (Fig. 5), suggest that the νCH increase could be attributed to a dispersion effect generated by WDF.

There is a slight, but non-significant decrease of the νCH intensity in going from sol to gel in the controls without fibre, this

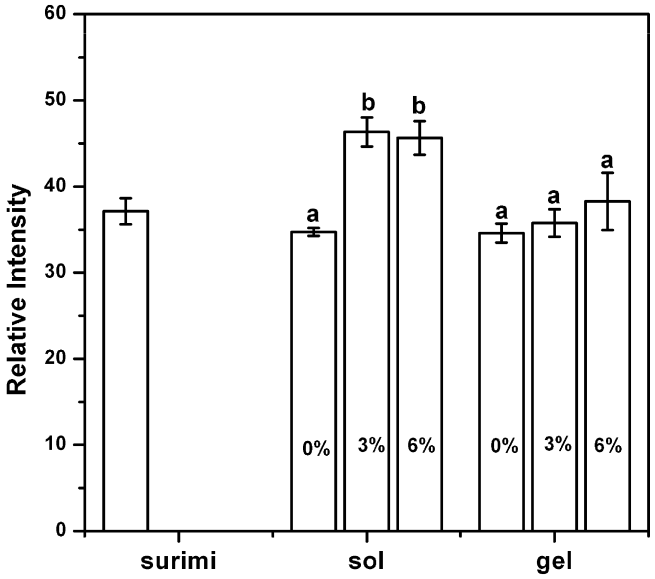

Fig. 8. Bar diagram corresponding to νCH relative intensities (I_{2935}/I_{1003}) during gelation with 0%, 3% and 6% WDF at 74.5% moisture content. Bars with different letters in the same phase mean significant differences ($P < 0.05$). Error bars indicate standard error of the mean.

decrease being more pronounced in the fibre-containing formulations (Fig. 8). It is well-known that hydrophobic interactions become stronger at increasing temperatures (Rader et al., 2002; Wang, Lin, Li, Wei, & Hsieh, 2005). One possible explanation for this differential behaviour between the fibre-containing and control formulations could be that some WDF-protein hydrophobic contacts, with subsequent νCH intensity decrease, occur.

No significant differences were observed for other tertiary structural details revealed by the tyrosine and tryptophan bands, indicative of variations of their local medium environment.

The results we have described here regarding to WDF-protein structural interactions are compatible with the changes in rheological and functional properties, and the ultrastructure of *surimi* gels with WDF (Sánchez-González, 2008), as well as the folding test. Raman results suggest that these differences may be caused by the dispersion effect of the fibre on the protein in the sol and a subsequent higher coagulation, with respect to gel formation during heating, as well as occurrence of hydrophobic contacts between the protein and fibre, leading to an impaired possibility of intermolecular protein crosslinks. In addition, Raman spectroscopy also suggests that the water released by the protein is taken by the WDF, which, either by acting as a dehydrating agent during heating, or by physically avoiding network formation as a consequence of dispersion, is the cause of this dehydration effect.

4. Conclusions

The Raman spectra of Vitacel wheat dietary fibre have been analysed here in terms of contributions of cellulose and hemicellulose. The spectra are dominated by bands of natural cellulose I, as the major component of WDF, and hemicellulose, being visible through some weak Raman signal, due to small concentration of this component.

We have shown that hydration of WDF involves νCH frequency upshifting and decreasing intensity, which can be explained in terms of formation of blue-shifting C–H···O hydrogen bonding between cellulose C–H bonds and water molecules. On this basis it is suggested that, when WDF is added to *surimi* for subsequent production of gels in the present experimental conditions, the local moisture of WDF within the gel phase is higher relative to the mean moisture of the whole samples.

WDF and heating together cooperatively act to generate β-sheets, which are attributed to nonspecific coagulation rather than network formation. Also, this dietary fibre produces changes in tertiary structure of proteins in the sol phase, manifested by changes in the environments of hydrophobic side chains, which become more solvent-exposed and, upon heating, may lead to hydrophobic contacts between the protein and fibre, as judged by the νCH decrease.

Acknowledgements

This work was performed within the Integrated Project SEAFOODplus, partially granted by the European Union under Contract No. 506359 and the Spanish Ministerio de Educación y Ciencia under Project AGL2006-26016-E/GAN. The authors A.R.-C. and I.S.-G. thank the CSIC for financing I3P Grants from CSIC (*European Social Foundation*). Thanks are due to Pilar Moreno for her excellent laboratory assistance.

References

Agarwal, U. P., & Ralph, S. A. (1997). FT-Raman spectroscopy of wood: Identifying contributions of lignin and carbohydrate polymers in the spectrum of black spruce (*Picea mariana*). *Applied Spectroscopy, 51*, 1648–1654.

Al-Azzam, W., Pastrana, E. A., Ferrer, Y., Huang, Q., Schweitzer-Stenner, R., & Griebenow, K. (2002). Structure of poly(ethylene glycol)-modified horseradish peroxidase in organic solvents: Infrared amide I spectral changes upon protein dehydration are largely caused by protein structural changes and not by water removal per se. *Biophysical Journal, 83*, 3637–3651.

Alix, A. J. P., Pedanou, G., & Berjot, M. (1988). Determination of the quantitative secondary structure of proteins by using some parameters of the Raman amide I band. *Journal of Molecular Structure, 174*, 159–164.

Barnes, A. J. (2004). Blue-shifting hydrogen bonds-are they improper or proper? *Journal of Molecular Structure, 704*, 3–9.

Bouraoui, M., Nakai, S., & Li-Chan, E. (1997). In situ investigation of protein structure in Pacific whiting *surimi* and gels using Raman spectroscopy. *Food Research International, 30*, 65–72.

Careche, M., Herrero, A., Rodríguez-Casado, A., Del Mazo, M. L., & Carmona, P. (1999). Structural changes of hake fillets: Effects of freezing and frozen storage. *Journal of Agricultural and Food Chemistry, 47*, 952–959.

Carmona, P., Molina, M., & Rodríguez-Casado, A. (2003). Raman study of the thermal behavior and conformational stability of basic pancreatic trypsin inhibitor. *European Biophysics Journal, 32*, 137–143.

Dreher, M. (2001). Dietary fibre overview. In S. Sungsoo-Cho & M. L. Dreher (Eds.), *Hand book dietary fibre* (pp. 1–217). New York: Marcel Dekker.

Gallaher, D. D. (2000). Dietary fibre and its physiological effects. In K. M. Schmidl & P. T. Labuza (Eds.), *Essentials of functional foods* (pp. 273–292). Maryland: Aspen Publishers Inc.

Gussoni, M., & Castiglioni, C. (2000). Infrared intensities. Use of the CH-stretching band intensity as a tool for evaluating the acidity of hydrogen atoms in hydrocarbons. *Journal of Molecular Structure, 521*, 1–18.

Herrero, A., Carmona, P., & Careche, M. (2004). Raman spectroscopic study of structural changes in hake muscle proteins during frozen storage. *Journal of Agricultural and Food Chemistry, 52*, 2147–2153.

Lanier, T., Hart, K., & Martin, R. (1991). *National Fisheries Institute. A manual of standard methods for measuring and specifying the properties of surimi*, Technical subcommittee of the *surimi* and *surimi* seafoods. Washington: National Fisheries Institute.

Lee, C. M. (2002). Role of hydrodynamically active biopolymer ingredients in texture modification and physical stabilization of gel-based products. *Journal of Food Science, 67*, 902–908.

Mizuno, K., Imafuji, S., Fujiwara, T., Ohta, T., & Tamiya, Y. (2003). Hydration of the CH groups in 1,4-dioxane probed by NMR and IR: Contribution of blue-shifting $H_2O\cdots$hydrogen bonds. *Journal of Physical Chemistry B, 107*, 3972–3978.

Niwa, E. (1992). Chemistry of *surimi* gelation. In T. C. Lanier & C. Lee (Eds.), *Surimi* technology (pp. 389–427). New York: Marcel Dekker.

Niwa, E., & Nakajima, G. (1975). Differences in protein structure between elastic kamaboko and brittle one. *Nippon Suisan Gakkaishi, 41*, 579.

Proniewicz, L. M., Paluszkiewick, C., Weseluch-Birczynska, A., Majcherczyk, H., Baranski, A., & Konieczna, A. (2001). FT-IR and FT-Raman study of hydrothermally degradated cellulose. *Journal of Molecular Structure, 596*, 163–169.

Rader, A. J., Hespenheide, B. M., Kuhn, L. A., & Thorpe, M. F. (2002). Protein unfolding: Rigidity lost. *Proceedings of the National Academy of Sciences of the United States of America, 99*, 3540–3545.

Robertson, J. A., & Eastwood, M. A. (1981). A method to measure the water-holding properties of dietary fibre using suction pressure. *British Journal of Nutrition, 46*, 247–255.

Sánchez-Alonso, I., Haki-Maleki, R., & Borderías, J. (2007). Wheat fibre as a functional ingredient in restructured fish products. *Food Chemistry, 100*, 1037–1043.

Sánchez-Alonso, I., Haki-Maleki, R., & Borderías, J. (2006). Effect of wheat fibre in frozen stored fish muscular gels. *European Food Research and Technology, 223*(4), 571–576.

Sánchez-González, I., Carmona, P., Moreno, P., Borderías, J., Sánchez-Alonso, I., Rodríguez-Casado, A., et al. (2008). Protein and water structural changes in *surimi* during gelation as revealed by H/D exchange and Raman spectroscopy. *Food Chemistry, 106*, 56–64.

Sánchez-González, I., In *structural and rheological study of surimi gel products with dietary fibres*. PhD Thesis. University Complutense of Madrid, Veterinary Faculty. Madrid 2008. Rheology of wheat dietary fibre enriched *surimi* gels.

Saura-Calixto, F., & Goñi, I. (2005). Fibra dietética y antioxidantes en la dieta española y en alimentos funcionales. In A. Olano, M. Juarez, & F. Morais (Eds.), *Alimentos funcionales*. Spain: Fundación Española para la Ciencia y Tecnología.

Shen, Q., Rahiala, H., & Rosenholm, J. B. (1998). Evaluation of the structure and acid-base properties of bulk wood by FT-Raman spectroscopy. *Journal of Colloid and Interface Science, 206*, 558–568.

Thawornchinsombut, S., Park, J. W., Meng, G. T., & Li-Chan, E. C. Y. (2006). Raman spectroscopy determines structural changes associated with gelation properties of fish proteins recovered at alkaline pH. *Journal of Agricultural and Food Chemistry, 54*, 2178–2187.

Van de Weert, M., Haris, P. I., Hennik, W. E., & Crommelin, D. J. A. (2001). Fourier transform infrared spectrometric analysis of protein conformation: Effect of sampling method and stress factor. *Analytical Biochemistry, 297*, 160–169.

Wang, S. L., Lin, S. I., Li, M. J., Wei, Y. S., & Hsieh, T. F. (2005). Temperature effect on the structural stability, similarity, and reversibility of human serum albumin in different states. *Biophysical Chemistry, 114*, 205–212.

Wiley, J. H., & Atalla, R. H. (1987). Band assignments in the Raman spectra of celluloses. *Carbohydrate Research, 160*, 113–129.

Zhbankov, R. G., Firsov, S. P., Buslov, D. K., Nikonenko, N. A., Marchewka, M. K., & Ratajczak, H. (2002). Structural physical-chemistry of cellulose macromolecules. Vibrational spectra and structure of cellulose. *Journal of Molecular Structure, 614*, 117–125.